

Iron Redox Cycling in Surface Waters: Effects of Humic Substances and Light

BETTINA M. VOELKER,^{*,†}
FRANÇOIS M. M. MOREL,[‡] AND
BARBARA SULZBERGER[†]

Swiss Federal Institute for Environmental Science and
Technology (EAWAG), Ueberlandstrasse 133, CH-8600
Duebendorf, Switzerland, and Geosciences Department,
Princeton University, Princeton, New Jersey 08540

The purpose of this study is to examine the mechanism of photo-oxidation of natural dissolved organic matter (DOM) in the presence of iron. This process is of interest in natural waters for several reasons: as a significant sink of DOM in sunlit surface waters; as a source and sink of reactive oxygen species ($\text{HO}_2/\text{O}_2^{\cdot-}$, hydrogen peroxide, and HO^{\cdot}) and as a factor controlling iron speciation. Studies were conducted in laboratory model systems containing fulvic acid and lepidocrocite ($\gamma\text{-FeOOH}$) particles at pH 3 and pH 5, irradiated with simulated sunlight. Measured concentrations of dissolved Fe(II), total dissolved Fe, and hydrogen peroxide were interpreted as the net effects of competing reactions reducing and oxidizing Fe and producing and destroying hydrogen peroxide. A kinetic model constructed using information gained from separate experiments in simpler systems was used to assess the relative importance of individual reactions. Comparison of photoreductive dissolution rates in aerated and de-aerated systems at pH 3 and pH 5 indicated that the decrease in rate with increasing pH is mostly due to a decrease in the concentration of surface Fe(III)–fulvate complexes and that, in the presence of oxygen, some of the surface Fe(II) is re-oxidized (not necessarily by oxygen) before detachment can take place. Kinetic modeling indicated that fast redox cycling of Fe occurs at both pH values. The dark reduction of Fe(III) by fulvic acid and photochemical ligand-to-metal charge transfer reactions of dissolved Fe(III)–fulvate complexes play almost equally significant roles in the reduction of dissolved Fe(III). The main oxidants of dissolved Fe(II) are $\text{HO}_2/\text{O}_2^{\cdot-}$ (produced via reduction of O_2 by photo-excited fulvic acid) and hydrogen peroxide [the product of Fe(II) reaction with $\text{HO}_2/\text{O}_2^{\cdot-}$].

Introduction

The cycling of iron between its reduced and oxidized forms and between particulate and dissolved species in natural waters has a number of environmental consequences beyond iron's role as a nutrient and as a sorbent. Iron photo-redox cycling has been shown to catalyze the oxidation of dissolved organic matter (1). This process could represent a significant sink of biologically refractory material (i.e., humic substances)

* Corresponding author's current address: Massachusetts Institute of Technology, Room 48-419, Cambridge, MA 02139; phone: (617) 253-3726; fax: (617) 258-8850; e-mail: voelker@mit.edu.

[†] EAWAG.

[‡] Princeton University.

and is closely coupled to the cycling of reactive transient species such as H_2O_2 , HO^{\cdot} , and $\text{HO}_2/\text{O}_2^{\cdot-}$ (2–7).

Our goal in this study is to gain a more thorough understanding of the mechanism of iron-catalyzed photo-oxidation of humic substances and of the effects of this process on iron speciation and on the fate of reactive transients, by attempting to account for all of the important reactions taking place in a model system. This laboratory study was conducted using a well-defined crystalline iron oxide phase (lepidocrocite or $\gamma\text{-FeOOH}$) and a standard humic substance (Suwannee River fulvic acid) in solutions at pH 3 and pH 5, with fulvic acid concentrations, iron concentrations, and light conditions chosen to be similar to those of acidic surface waters. [Because of the increased rates of Fe(II) oxidation reactions with increasing pH, experiments could not be conducted at neutral and higher pH values.]

A general description of iron redox cycling in the presence of humic substances and light must include both iron redox reactions of dissolved Fe species and those taking place on the surface of the iron oxide particles as well as the transfer of iron species from the surface to the solution and vice versa. These processes are summarized in Figure 1 and are described below.

Photo-Reduction of Dissolved Fe(III) by Fulvic Acid. The mechanism of photochemical iron reduction (reaction 1 in Figure 1) by humic substances is thought to proceed by a mechanism similar to that observed for simple Fe(III)–carboxylate complexes, such as citrate (8), oxalate (2), or malonate (3). Absorption of a photon results in an excited, ligand-to-metal charge transfer (LMCT) state of the complex, which either may be thermally de-activated or may dissociate. In the latter case, Fe(II) and an oxidized organic radical are formed (9). This primary radical may undergo decarboxylation to form a secondary, carbon-centered radical and CO_2 (3). If the primary or secondary radicals are reductants, a second Fe(III) will be reduced to Fe(II), or oxygen, if present, will be reduced to superoxide radical ($\text{HO}_2/\text{O}_2^{\cdot-}$). This is generally the case if the organic radical can form a stable oxidized product by elimination of a single electron (for example oxalate, α -hydroxy or α -amino carboxylic acids; 2, 10, 11). The observed yield of Fe(II) per carboxylate ligand oxidized may therefore be as high as 2 in de-aerated systems and is expected to be 1 or less in aerated systems (because O_2 , $\text{HO}_2/\text{O}_2^{\cdot-}$, and its dismutation product H_2O_2 will all re-oxidize some Fe(II)—see ref 3 and below).

Little is known about the organic products of Fe(III)–humate LMCT reactions. Reactions of organic radicals with each other may result in further polymerization of the humic material, though perhaps not in the presence of oxygen. Peroxyl radicals can be formed by the addition of oxygen to carbon-centered radicals. These may react with each other in termination reactions to form non-radical and non-peroxidic products or may abstract hydrogen from other organic compounds to generate organic peroxides and new organic radicals (11, 12). Both peroxyl radicals and organic peroxides could also oxidize Fe(II).

Photo-Reductive Dissolution of Iron(III) Oxide. Humic substances or other carboxylate ligands can form surface Fe(III)–carboxylate complexes which, like dissolved complexes, are also thought to participate in LMCT reactions (reaction 2 in Figure 1; 8, 9, 13, 14). For photo-reductive dissolution to take place, the Fe(II) formed at the surface of the iron(III) oxide must then detach (reaction 3 in Figure 1). In the presence of oxidants, for example, O_2 , the surface Fe(II) may be re-oxidized before it can detach (reaction 4 in Figure 1). Because the rate of oxidation of surface Fe(II) is much faster than that of dissolved Fe^{2+} (15), this reaction may be

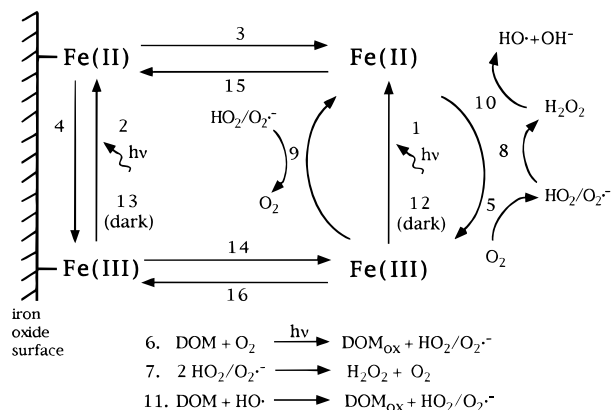
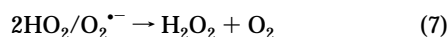


FIGURE 1. Schematic summary of possible iron reactions in surface waters: (1) photo-reduction of dissolved Fe(III) by DOM, (2) photo-reduction of surface Fe(III) by DOM, (3) detachment of surface Fe(II), (4) re-oxidation of surface Fe(II), (5) Fe(II) oxidation by O_2 , (6) $\text{HO}_2/\text{O}_2^{\cdot-}$ photoproduction, (7) bimolecular dismutation of $\text{HO}_2/\text{O}_2^{\cdot-}$, (8) Fe(II) oxidation by $\text{HO}_2/\text{O}_2^{\cdot-}$, (9) Fe(III) reduction by $\text{HO}_2/\text{O}_2^{\cdot-}$, (10) Fe(II) oxidation by H_2O_2 , (11) regeneration of $\text{HO}_2/\text{O}_2^{\cdot-}$ from $\text{HO}\cdot$, (12) Fe(III) dark reduction by DOM, (13) dark reduction of surface Fe(III) by DOM, (14) non-reductive dissolution of Fe(II) oxide, (15) sorption of dissolved Fe(II), (16) Fe(III) adsorption/precipitation.

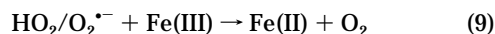
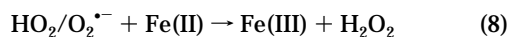
important under solution conditions where the rate of oxidation of dissolved Fe(II) is insignificant. Depending on the rate of detachment versus the rate of re-oxidation, LMCT reactions at the surface of iron oxides may therefore lead to little or no photo-reductive dissolution of iron, even though the ligand is still oxidized (16). (Other mechanisms for Fe reduction and ligand oxidation taking place at iron oxide surfaces are also possible; see Discussion.)

Photo-Formation of Fe(II) Oxidants. Within the acidic pH range considered in this study, the oxidation of dissolved Fe(II) by oxygen (reaction 5 in Figure 1) is expected to be very slow compared to other processes. However, the irradiation of humic substances in the presence of oxygen results in the formation of $\text{HO}_2/\text{O}_2^{\cdot-}$ (reaction 6 in Figure 1) (11, 17–19). The mechanism of this reaction is not known but may occur via reduction of O_2 by aqueous electrons or triplet states, both formed when humic substances are photo-excited. A possible additional source of $\text{HO}_2/\text{O}_2^{\cdot-}$ is the reduction of O_2 by the primary photooxidation product of ligand-to-metal charge-transfer reactions of Fe(III)–humate complexes (see above).

The end product of $\text{HO}_2/\text{O}_2^{\cdot-}$ dismutation ($\text{p}K_a$ 4.8; 20) is hydrogen peroxide, by the following reaction (numbering of reactions in the text continues the numbering in Figure 1):



This reaction is catalyzed in the presence of dissolved Fe by the reactions:



In the presence of a high flux of $\text{HO}_2/\text{O}_2^{\cdot-}$, a steady-state ratio of Fe(II) and Fe(III) is established, so that reactions 8 and 9 proceed at equal rates. In this case, the overall stoichiometry of $\text{HO}_2/\text{O}_2^{\cdot-}$ dismutation is equal to that in reaction 7: 0.5 mol of hydrogen peroxide is formed for every mole of $\text{HO}_2/\text{O}_2^{\cdot-}$ consumed. However, if the flux of $\text{HO}_2/\text{O}_2^{\cdot-}$ is small as compared to the concentration of either Fe(II) or Fe(III), or if other reactions of Fe(II) and Fe(III) prevent the steady-state ratio from being reached, the stoichiometry of hydrogen peroxide formation could be anything between 1 (if reaction

8 dominates) and 0 (if reaction 9 dominates) mol of hydrogen peroxide formed per mol of $\text{HO}_2/\text{O}_2^{\cdot-}$ consumed. The former case is expected in systems containing micromolar concentrations of Fe(II) and fulvic acid; reaction 9 is likely to be negligible because of the formation of Fe(III)–humate complexes, which, like other carboxylate complexes (6, 20), probably react more slowly with $\text{O}_2^{\cdot-}$ than inorganic Fe(III) (21). Neither bimolecular dismutation (reaction 7) nor catalyzed dismutation (analogous to reactions 8 and 9) by other metals present at contaminant levels should be fast enough to outcompete micromolar concentrations of Fe(II) for $\text{HO}_2/\text{O}_2^{\cdot-}$. Reactions of $\text{HO}_2/\text{O}_2^{\cdot-}$ with organic compounds also tend to be slow and generally do not lead to hydrogen peroxide formation (20).

The hydrogen peroxide formed from $\text{HO}_2/\text{O}_2^{\cdot-}$ is another potentially significant oxidant of Fe(II) (Fenton's reaction, reaction 10 in Figure 1). The kinetics of oxidation of Fe(II) by hydrogen peroxide in the presence of fulvic acid have been studied in detail in our previous work (7). In the presence of oxygen, some of the $\text{HO}\cdot$ produced by this reaction was found to react with fulvic acid to regenerate $\text{HO}_2/\text{O}_2^{\cdot-}$ (reaction 11 in Figure 1).

Other Processes. Additional (non-photochemical) processes that need to be considered in this system are the dark reduction of Fe(III) (reaction 12 in Figure 1) (7), thermal reductive dissolution of iron(III) oxide (reaction 13 in Figure 1) by humic substances (22), dissolution of iron(III) oxide via non-reductive processes (reaction 14 in Figure 1) (23), adsorption of Fe(II) to iron oxide surfaces (reaction 15 in Figure 1) (8), and removal of dissolved Fe(III) by precipitation (reaction 16 in Figure 1).

Materials and Methods

Acid-washed glassware and reagent-grade chemicals were used in all experiments. Solutions of Suwannee River fulvic acid (SRFA) (obtained from J. Leenheer; 24) were prepared fresh every month and stored in the refrigerator. Lepidocrocite was synthesized by slow oxidation of Fe(II) near neutral pH (25) and stored in suspension in a polypropylene bottle kept in the dark at 4 °C. The identity of the product was verified using FTIR spectroscopy. The same batch of lepidocrocite was used in all of the experiments.

Chemical kinetic calculations were performed using the program Acuchem (26). Kinetic parameters optimizing the fit of a kinetic model to the data were determined using a simplex routine in the mathematics software package Matlab (27).

Analysis of Fe and H_2O_2 . Aliquots of the lepidocrocite suspensions were filtered (acid-rinsed 0.1 μm cellulose nitrate filters) before dissolved Fe(II), total dissolved Fe, and hydrogen peroxide were measured as described previously (27, 28). For measurement of total Fe in the suspensions, 1 mL of an unfiltered solution sample was mixed with 1 mL of the reducing reagent and left to stand for at least 48 h before addition of ferrozine and buffer.

Adsorption Isotherms. Lepidocrocite was added from a stock suspension to solutions of varying concentrations of fulvic acid, stirred overnight (20–22 °C) and then centrifuged (10 000 rpm, 20 min). Fulvic acid concentration in the supernatant was determined by comparing the absorption spectrum to that of a reference solution of 10 mg/L fulvic acid (300–600 nm). The shape of the spectrum in the supernatant was not significantly different from that in the reference solution, indicating that preferential adsorption of some fraction of the fulvic acid did not take place. No loss of fulvic acid was observed in controls without added lepidocrocite.

At pH 5, centrifugation was not sufficient to remove all the lepidocrocite from the supernatant. Small concentrations of these particles had a significant effect on the absorption spectra. To minimize this problem, the supernatant was

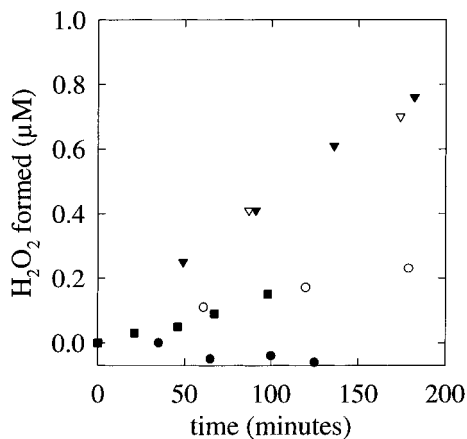


FIGURE 2. Comparison of photo-formation rate of hydrogen peroxide under various conditions. All systems contained 10 mg/l fulvic acid and were irradiated beginning at $t = 0$. (∇) aerated, pH 3; (\blacktriangledown) aerated, pH 5; (\bullet and \circ) de-aerated, pH 3; (\blacksquare) aerated in the presence of $\text{NO}_{(\text{aq})}$, pH 3.

filtered ($0.45 \mu\text{m}$, cellulose nitrate) after centrifugation. Since small amounts of fulvic acid were found to be removed by the filter ($<5\%$), spectra were compared to a reference spectrum of a solution of 10 mg/L fulvic acid that had also been filtered. Interaction of fulvic acid with the filter or with lepidocrocite particles on the filter may be the cause of the higher scatter observed in the data at pH 5.

Kinetic Experiments. Experiments were carried out at 25°C in a 300-mL Pyrex reactor equipped with a water jacket. All solutions contained 10 mM NaClO_4 and 10 mg/L SRFA and were stirred vigorously. The pH was adjusted with HClO_4 or NaOH . Lepidocrocite was added to solutions from a stock suspension and left to condition overnight in the dark before experiments were started. Aerated solutions were bubbled with synthetic air (20% $\text{O}_2/80\% \text{N}_2$) prior to and during the experiments. When de-aerated solutions were prepared, the air in the headspace of the reactor was first removed by connecting the reactor to a vacuum pump. The headspace was then filled with nitrogen gas that had first been scrubbed of trace amounts of oxygen with a Jones reductor (29). This procedure was repeated several times. Solutions were then continuously purged with scrubbed nitrogen gas. Solutions containing NO were bubbled with a 1000 ppm NO/N_2 mixture (aerated solutions were simultaneously bubbled with the synthetic air mixture) for several hours prior to and during the experiment. Solutions were irradiated with white light by a 1000-W high-pressure xenon lamp (OSRAM) through a quartz window on the bottom of the reactor (30).

Photo-dissolution experiments were repeated several times; observed dissolution rates did not vary significantly (less than 10%, normalized to total particulate Fe) from one experiment to the next.

Actinometry. We measured the average incident light intensity on the reaction vessel through a narrow band filter (transmission maximum at 436 nm) using ferrioxalate actinometry. The total light intensity hitting the vessel in our experiments, when the light was not filtered, could then be calculated from the value of the photon flux of the filtered light, the transmission spectrum of the filter, and the spectrum of unfiltered light. At the power setting used for all experiments, the incident light intensity on the reaction vessel was calculated to be 0.5 kW m^{-2} or approximately half the intensity of sunlight at mid-latitude solar noon (27). The experiments shown in Figure 2 were performed with a different setup of the optical bench and, therefore, represent slightly different light conditions (approximately 40% higher light intensity than in the other experiments).

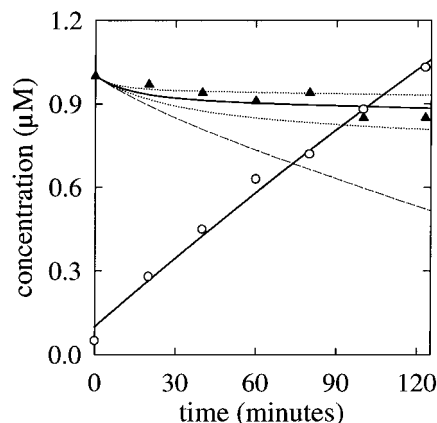


FIGURE 3. Formation of hydrogen peroxide (\circ) and oxidation of $\text{Fe}(\text{II})$ (\blacktriangle) in an irradiated 10 mg/L SRFA solution at pH 3 containing initially $1.00 \mu\text{M}$ $\text{Fe}(\text{II})$. Lines show the results of kinetic model calculations (see text and Table 1).

Results

Many of the competing reactions occurring in our irradiated iron oxide/fulvic acid systems cannot be studied in isolation, and the concentrations of a number of the relevant species [for example, surface $\text{Fe}(\text{II})$ and $\text{HO}_2/\text{O}_2^{\cdot-}$] cannot be measured. To determine which reactions are likely to be most important and to obtain an estimate of their rates, we performed a series of experiments with increasingly complex systems and at each step interpreted the result with the help of a kinetic model.

Photo-Formation of Oxidants. In the absence of added Fe, the formation rate of hydrogen peroxide in an irradiated aerated solution of 10 mg/L SRFA is the same at pH 3 and pH 5 and remains constant over several hours (∇ and \blacktriangledown symbols in Figure 2). No formation or very slow formation of hydrogen peroxide is observed in de-aerated solutions (\bullet and \circ symbols in Figure 2). In the presence of $\text{NO}_{(\text{aq})}$, an $\text{HO}_2/\text{O}_2^{\cdot-}$ scavenger (7, 31, 32), the formation rate of hydrogen peroxide also slows down considerably (\blacksquare symbols in Figure 2). The kinetic modeling of this system is trivial, consisting only of a constant rate of production of $\text{HO}_2/\text{O}_2^{\cdot-}$ and hydrogen peroxide. (The exact stoichiometry of the rapid formation of hydrogen peroxide from $\text{HO}_2/\text{O}_2^{\cdot-}$ depends on whether the fate of $\text{HO}_2/\text{O}_2^{\cdot-}$ is governed by bimolecular dismutation or by reactions with metal contaminants.)

Photo-Redox Cycling of Dissolved $\text{Fe}(\text{III})$. To examine the redox cycling of dissolved Fe in the presence of light in aerated systems, we irradiated a solution at pH 3 containing 10 mg/L fulvic acid and an initial concentration of $1 \mu\text{M}$ $\text{Fe}(\text{II})$. As can be seen in Figure 3, little net oxidation of the $\text{Fe}(\text{II})$ took place. To understand why, we make use of a kinetic model including a number of competing iron redox reactions: oxidation of $\text{Fe}(\text{II})$ by $\text{HO}_2/\text{O}_2^{\cdot-}$, oxidation of $\text{Fe}(\text{II})$ by hydrogen peroxide, dark reduction of $\text{Fe}(\text{III})$, and photoreduction of $\text{Fe}(\text{III})$ (reactions 6, 8, and 10–12 in Figure 1 and Table 1).

To model our data, we assume that $\text{HO}_2/\text{O}_2^{\cdot-}$ is photo-produced at a constant rate throughout the experiment and that all of the $\text{HO}_2/\text{O}_2^{\cdot-}$ formed reacts immediately with $\text{Fe}(\text{II})$ to form $\text{Fe}(\text{III})$ and hydrogen peroxide (reaction 8 in Figure 1). The rate of photochemical formation of hydrogen peroxide by fulvic acid measured in Figure 2 cannot be used to derive an $\text{HO}_2/\text{O}_2^{\cdot-}$ formation rate in the presence of iron, because we are not certain of the stoichiometry of hydrogen peroxide formation from $\text{HO}_2/\text{O}_2^{\cdot-}$ in the absence of added iron and because additional $\text{HO}_2/\text{O}_2^{\cdot-}$ may be produced from LMCT reactions of $\text{Fe}(\text{III})$ -fulvate complexes. [The light conditions were also slightly different in the two experiments.] The rate of $\text{HO}_2/\text{O}_2^{\cdot-}$ formation (reaction 6) is therefore a fitting

TABLE 1. Reactions and Kinetic Parameters Used To Model Data Sets^a

reaction ^b	type of parameter (units)	pH 3, no γ -FeOOH (Figure 3)	pH 3 (Figure 6a)	pH 5 (Figure 6b)
(1) photoreduction of dissolved Fe(II)	first-order rate constant (s^{-1})	9.3×10^{-4} (best fit, solid line) 0 (dashed line) 4.5×10^{-4} (dotted line) 1.8×10^{-3} (dotted line)	2.8×10^{-4} (best fit, solid line) 3.6×10^{-4} (dotted line) 2.1×10^{-4} (dashed line)	3.5×10^{-4} (best fit, solid line) 4.3×10^{-4} (dotted line) 2.5×10^{-4} (dashed line)
(3) formation of dissolved Fe(II) from iron oxide phase; arbitrarily fit to tot. diss. Fe = $A(1 - \exp(-Bt))$	A (μM) B (s^{-1})		6.74×10^{-6} 9.68×10^{-5}	2.11×10^{-6} 1.46×10^{-4}
(6) $HO_2/O_2^{\cdot-}$ photoforformation	rate ($M s^{-1}$)	1.42×10^{-10}	1.40×10^{-10} (best fit, solid line) 1.60×10^{-10} (dotted line) 1.20×10^{-10} (dashed line)	1.41×10^{-10} (best fit, solid line) 1.60×10^{-10} (dotted line) 1.20×10^{-10} (dashed line)
(8) $Fe(II) + HO_2/O_2^{\cdot-} \rightarrow Fe(III) + H_2O_2$	assumed instantaneous			
(10) $Fe(II) + H_2O_2 \rightarrow Fe(III) + OH^- + HO^{\cdot}$	overall second-order rate constant ($M^{-1} s^{-1}$)	49.8 ^c		176.2 ^c
(11) $HO_2/O_2^{\cdot-}$ from HO^{\cdot}	yield (%)	47.6 ^c		36.3 ^c
(12) dark reduction of Fe(III) (rapid reduction step)	ratio (dimensionless)	0.31 ^d		0.19 ^d

^a All other reactions involving dissolved species were assumed to be insignificant. ^b Reaction numbers are the same as those used in Figure 1 and the text. ^c Effective rate constant in the presence of 10 mg/L Suwannee River fulvic acid (7). ^d See Table 1 of ref 7 for details and other reactions and kinetic parameters relating to Fe(III) reduction by fulvic acid.

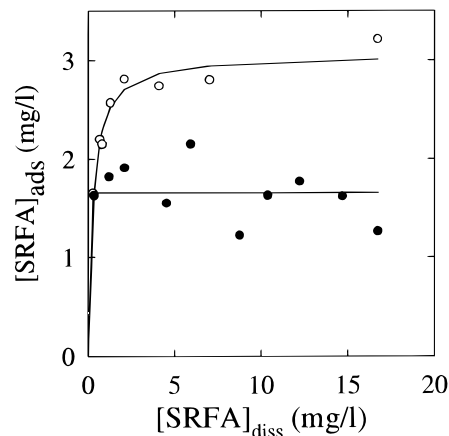


FIGURE 4. Adsorbed versus dissolved fulvic acid concentration at pH 3 (○) and pH 5 (●) in lepidocrocite suspensions (approximately 450 μM total Fe). The saturation concentration was determined at pH 3 using a fit of the data to the Langmuir equation and at pH 5 by averaging the concentration of adsorbed fulvic acid (solid lines).

parameter in the model, well-constrained by the measured hydrogen peroxide formation rate.

The effective second-order rate constant for the oxidation of Fe(II) by hydrogen peroxide in the presence of fulvic acid (reaction 10) and the yield of $HO_2/O_2^{\cdot-}$ per HO^{\cdot} formed were determined in ref 7 and are also included in our model (reaction 11).

The kinetics of dark reduction of dissolved Fe(III) by fulvic acid (reaction 12) are quite complicated, but because the conditions of the experiments described here (pH, concentration ranges, time scale of experiments) are close to those of the experiments described in our previous work (7), the empirical description presented in that work should be directly applicable. For simplicity, we ignore the dependence of the extent of the initial rapid reduction step on the Fe(II) concentration, using a constant value corresponding to a total iron concentration of 1.5 μM .

A kinetic model calculation including all of these reactions but no Fe(III) photo-reduction (reaction 1) predicts far more Fe(II) oxidation than is actually observed (dashed line in Figure 3). If we include photoreduction with an effective first-order rate constant of $9.3 \times 10^{-4} s^{-1}$ (determined as the parameter that gave the best fit of the data), we obtain an adequate description of the behavior of Fe(II) (solid line in Figure 3). Results of the same calculation using rate constants of $4.5 \times 10^{-4} s^{-1}$ and $18 \times 10^{-4} s^{-1}$ (dotted lines in Figure 3) give us a reasonable error estimate on this parameter of a factor of 2. This experiment then provides us with evidence that photoreduction of dissolved Fe(III) by fulvic acid must be proceeding at a significant rate.

Photo-Reductive Dissolution of γ -FeOOH by Adsorbed Fulvic Acid. Adsorption isotherms of fulvic acid on the lepidocrocite surface show that, at both pH 3 and pH 5, the concentrations of adsorbed fulvic acid as a function of dissolved fulvic acid rise steeply and reach a plateau at very low concentrations (Figure 4). The saturation concentration of humic substances on an iron oxide surface apparently decreases with increasing pH, as has previously been observed (29). From these data, we can calculate the saturation concentration of adsorbed fulvic acid as $6.8(\pm 0.4) \times 10^{-6} g$ of SRFA/ μM Fe at pH 3 (using a least-squares fit of the Langmuir equation) and $3.7(\pm 0.4) \times 10^{-6} g$ of SRFA/ μM Fe at pH 5 (taking the average of the $[SRFA]_{ads}$ values shown) (solid lines in Figure 4). Under the conditions of the reductive dissolution experiments, in the presence of 10 mg/L SRFA and 45 μM Fe as γ -FeOOH, the fulvic acid is present in great excess of the available surface sites. We expect 0.31 (± 0.02) mg/L of the total fulvic acid to be adsorbed at pH 3 and 0.17 (± 0.02) mg/L at pH 5. (Errors were estimated as 2σ .)

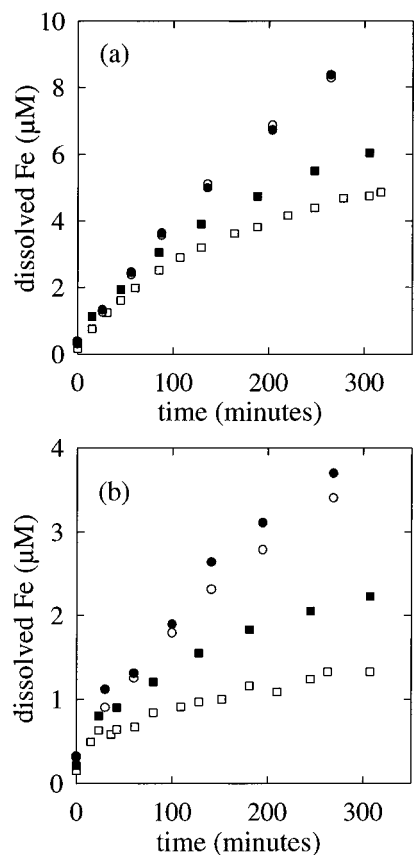


FIGURE 5. (a) Reductive dissolution of lepidocrocite in de-aerated (circles) and aerated (squares) solutions of 10 mg/L fulvic acid at pH 3 (Fe_T 40 μ M). Filled symbols represent total dissolved Fe concentrations; open symbols are Fe(II). (b) Same as panel a except at pH 5. Fe_T 45 μ M Fe (deaerated system) and 50 μ M (aerated system).

The rate of formation of dissolved iron by photo-reductive dissolution of lepidocrocite in the presence of 10 mg/L Suwannee River fulvic acid (SRFA) is strongly affected by both pH and the presence of oxygen (Figure 5). Almost no dissolution takes place during the time that the solutions are kept in the dark (14–19 h before time zero shown in Figure 5), demonstrating that dark dissolution processes (either reductive or non-reductive) are not significant in our systems.

In the absence of oxygen, the formation rate of dissolved Fe is approximately constant over time, and no formation of dissolved Fe(III) [measured as the difference between total Fe and Fe(II)] is observed.

In the presence of oxygen, the rate of formation of total dissolved Fe is decreased at both pH 3 and pH 5 and is no longer constant over time (Figure 5). Some formation of dissolved Fe(III) is also observed, due to re-oxidation of dissolved Fe(II). Under some conditions, dissolved Fe(III) could re-precipitate; this would result in a decrease in the observed net formation rate of dissolved iron. However, we have observed that micromolar concentrations of added dissolved Fe(III) remain filterable in solutions at pH 3 and pH 5 containing 10 mg/L SRFA and 40 μ M γ -FeOOH (27). Loss of Fe(II) due to adsorption or (possibly surface-catalyzed) Fe(II) oxidation by oxygen in lepidocrocite suspensions kept in the dark was also observed to be insignificant (27). The overall decrease in the rate of formation of dissolved Fe must therefore be due to a decrease in the rate of photoreductive dissolution in the presence of oxygen.

While dissolved Fe(II) and Fe(III) accumulate when aerated lepidocrocite suspensions are irradiated in the presence of fulvic acid, the concentration of hydrogen peroxide levels off after some time, both at pH 3 and at pH 5 (Figure 6). (No hydrogen peroxide formation is observed in the de-aerated suspensions—data not shown).

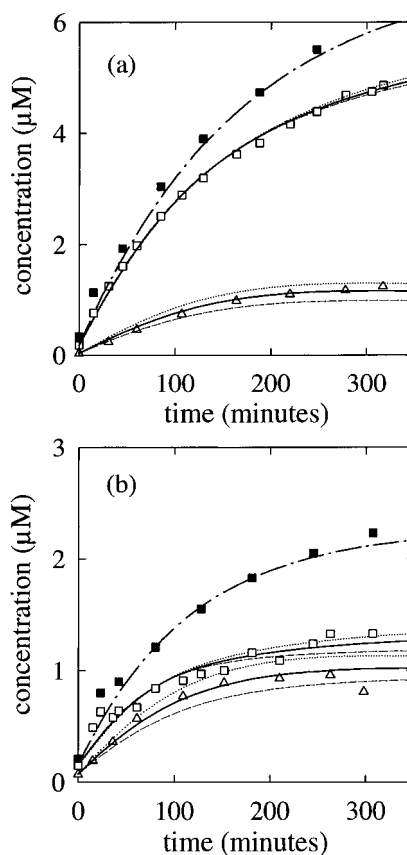


FIGURE 6. (a) Total dissolved Fe (■), Fe(II) (□), and hydrogen peroxide (△) in the aerated, irradiated lepidocrocite suspension at pH 3 (Fe_T 40 μ M). Dashed-dotted lines represent the modeled iron oxide photo-dissolution rate. Solid lines represent best model fit of the Fe(II) and hydrogen peroxide data; calculations using other model parameter values are also shown (see text and Table 1). (b) Same as panel a except at pH 5 (Fe_T 50 μ M).

Kinetics of Iron Redox Cycling in the Irradiated Lepidocrocite–Fulvic Acid System. In our model of this system (Table 1), we assume that the only addition to the reactions considered in the model for the homogeneous system (Figure 3) is an input of dissolved Fe(II) from the iron oxide surface (reaction 3). By comparing the values of the fitting parameters obtained in modeling this system with those obtained earlier (corrected for differences in light conditions due to absorption of light by the lepidocrocite), we can evaluate whether our model is sufficient or whether additional reactions must be considered in the heterogeneous system (for example, formation of $HO_2/O_2^{\cdot-}$ or destruction of hydrogen peroxide at the iron oxide surface).

The rate of Fe(II) input must be given by the rate of formation of total dissolved iron at each pH, because the rates of other surface-solution processes (reactions 12–15) were found to be insignificant. This rate is not constant at either pH, and an empirical function (total dissolved Fe = $A(1 - \exp(-Bt))$, where A and B are constants and t is time) is used to reproduce the observed accumulation of dissolved Fe as a function of time (Table 1, dashed-dotted lines in Figure 6).

Best values of the two fitting parameters [the rate constant for photo-reduction of dissolved Fe(III) and the rate of formation of $HO_2/O_2^{\cdot-}$] were again determined at each pH using the computer optimization routine described in the Materials and Methods section; these are listed in Table 1. The model accurately accounts for the behavior of Fe(II) and hydrogen peroxide at both pH values (solid lines in Figure 6). To demonstrate the sensitivity of the modeling procedure, results of calculations using slightly different pairs of values

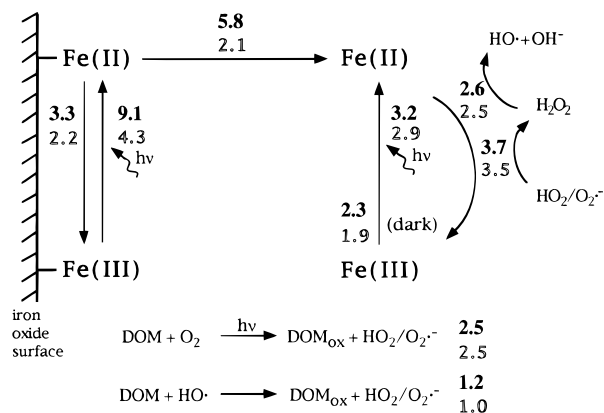


FIGURE 7. Summary of iron redox and surface reactions in aerated solutions containing lepidocrocite and fulvic acid (experiments shown in Figures 4 and 6). The numbers in italics indicate the amount of iron (in μM) oxidized or reduced by each of the depicted processes after 300 min of illumination at pH 3 (top numbers) and at pH 5 (bottom numbers). The rate of photo-reduction of surface Fe(III) was assumed to be equal to the rate of photo-reductive dissolution in de-aerated solutions. The amount of surface Fe(II) that re-oxidized instead of detaching was calculated as the difference in the amount of dissolved Fe (normalized to total iron oxide concentration) formed in the de-aerated and aerated solutions.

of the fitting parameters are also shown (dotted and dashed lines in Figure 6). These were obtained by increasing or decreasing the rate of $\text{HO}_2/\text{O}_2^{\cdot-}$ formation by 15% and then using the computer routine to determine the best value of the rate constant for photo-reduction of dissolved Fe(III). The fits obtained in this way are visibly poorer than those obtained by the simultaneous optimization of both parameters. Although a rigorous calculation of confidence limits for the fitting parameters cannot be made, this calculation suggests that the error is smaller than $\pm 15\%$.

We can compare the relative importance of competing processes by using the model to calculate the amount of Fe reduced or oxidized by each reaction (Figure 7). This calculation demonstrates that dissolved Fe(II) and Fe(III) are cycled back and forth rapidly and that this redox cycling is not dominated by only one or two reactions. Both light and dark reduction by fulvic acid play significant roles, and both hydrogen peroxide and $\text{HO}_2/\text{O}_2^{\cdot-}$ are important oxidants.

Discussion

The success of our models suggests that we have not neglected a significant source or sink of hydrogen peroxide, $\text{HO}_2/\text{O}_2^{\cdot-}$, or reduced iron. However, the adjustable parameters in the models could compensate for a mistaken assumption to some degree. In this section, we discuss what information the models provide concerning the individual reactions taking place in our experiments and whether the values of the fitting parameters obtained from the modeling are reasonable.

Photo-Reduction of Dissolved Fe(III). The effective first-order rate constant of photochemical ligand-to-metal charge transfer is a function of the amount of light absorbed by the complex and the quantum yield of the charge-transfer reaction and, therefore, depends on both light intensity and intrinsic properties of the complex. One might expect that different polycarboxylic acids resemble each other in these properties. The first-order rate constant for photochemical Fe(III) reduction determined in the lepidocrocite-free system, $9 \times 10^{-4} \text{ s}^{-1}$, corresponds to a half-life of the Fe(III)–SRFA complex on the order of 10 min at midlatitude solar noon. This is comparable to half-lives for Fe(III) complexes with malonate and citrate, estimated to be 5 and 0.9 min, respectively (3). The half-life of Fe(III)–aquo complexes under similar light conditions is approximately 9 min at pH 3 but 460 min at pH 5 (34).

The rate of photochemical iron reduction through the LMCT reaction should be pH independent as long as the same Fe complex is present at both pH values (2, 8). The values obtained from the kinetic model of the experiments in the presence of particles ($2.8 \times 10^{-4} \text{ s}^{-1}$ at pH 3 and $3.5 \times 10^{-4} \text{ s}^{-1}$ at pH 5) are roughly consistent with these expectations. The smaller values of the rate constant compared to the value obtained in the particle-free system (approximately $9 \times 10^{-4} \text{ s}^{-1}$) is consistent with the decrease in available light in the heterogeneous system.

Photo-Reductive Dissolution of Iron(III) Oxide. A decrease in the rate of reductive dissolution with increasing pH has been observed for a number of ligands (8, 16, 35) and is usually attributed to a decrease in the amount of ligand adsorbed. If we assume that the fulvic acid has an average molecular mass of 800 DA (36) and that each adsorbed fulvic acid molecule forms a 1:1 complex with surface Fe(III), then the concentration of surface Fe(III) complexes is $3.9 (\pm 0.2) \times 10^{-7} \text{ M}$ in the de-aerated system at pH 3 and $2.1 (\pm 0.2) \times 10^{-7} \text{ M}$ in the de-aerated system at pH 5 (Figure 4). The dissolution rates (from linear least square fits of the total Fe data in deaerated suspensions, Figure 4) are $5.0 (\pm 0.4) \times 10^{-10} \text{ M s}^{-1}$ and $2.1 (\pm 0.3) \times 10^{-10} \text{ M s}^{-1}$ at pH 3 and pH 5 respectively, leading to overall apparent first-order rate constants of $1.4 (\pm 0.1) \times 10^{-3} \text{ s}^{-1}$ (pH 3) and $1.0 (\pm 0.2) \times 10^{-3} \text{ s}^{-1}$ (pH 5) in the de-aerated lepidocrocite suspensions. The slight effect of pH on the rate constants could be due to a pH dependence of surface Fe(II) detachment rates, leading to an accumulation of Fe(II) on the surface of the iron oxide and therefore a blocking of surface sites for reductive dissolution (16). However, the effect in our systems is much smaller than that observed for the photo-reductive dissolution of lepidocrocite in the presence of oxalate where the overall rate constant was found to vary with $[\text{H}^+]^{0.27}$ (16).

The apparent first-order rate constant of the surface Fe(III)–SRFA complex is of the same order of magnitude as the apparent constant measured by Waite and Morel (8) for surface citrate complexes on lepidocrocite, $3.5 \times 10^{-3} \text{ s}^{-1}$. Their light source produced a spectrum close to ours, but with a total light intensity approximately twice as high. However, this dissolution rate was measured in aerated systems and could represent an underestimate of the actual amount of iron photo-reduced at the surface. Like Waite and Morel, we observe that the apparent rate constants for the surface and solution complexes are of similar magnitude.

Photo-reductive dissolution processes involving oxidation of organic ligands may also proceed by other mechanisms besides the LMCT reactions discussed here: a semiconductor mechanism where the adsorbed ligand is oxidized by photoholes and surface Fe(III) is reduced by photoelectrons (35, 37) and a direct electron transfer mechanism (38). In theory, comparison of the wavelength dependence of the rate of photo-reductive dissolution with the absorption spectra of the different chromophores involved in these different mechanisms should enable one to distinguish among the mechanisms. However, because in our system the absorption spectra of the adsorbed species are obscured by those of the bulk phases (the iron oxide and dissolved fulvic acid) such comparison is not feasible. Furthermore, it is not clear that either the dependence of the rate on the quantity of ligand adsorbed or the products should be different if the reaction proceeded by a mechanism other than ligand-to-metal charge transfer (37).

The decrease in the rate of photo-reductive dissolution in the presence of oxygen at both pH 3 and pH 5 (Figure 4) indicates oxidation of some of the surface-bound Fe(II) before detachment can take place. The decrease in the rate of formation of dissolved Fe over time seems to imply that the oxidant is accumulating over time and is therefore not oxygen. Hydrogen peroxide is a possibility (39), but this implies a sink of several micromolar of hydrogen peroxide [corresponding

to the amount of surface Fe(II) oxidized] during our experiments, inconsistent with our kinetic model. Another possibility is organic peroxides or other reasonably stable organic oxidants formed as byproducts of photo-oxidation reactions.

Formation of Fe(II) Oxidants. Hydrogen peroxide photo-formation is inhibited both in the presence of $\text{NO}_{(\text{aq})}$ and when oxygen is thoroughly eliminated from the solution (Figure 2). This is consistent with previous workers' conclusions (11, 17–19) that most or all of the hydrogen peroxide is formed via reduction of O_2 to $\text{O}_2^{\cdot-}$ by the photo-excited fulvic acid. (A slow buildup of hydrogen peroxide is sometimes observed in de-aerated solutions, presumably because of contaminating traces of O_2 .) The small production rate of hydrogen peroxide that was observed in the presence of $\text{NO}_{(\text{aq})}$ probably indicates that NO was not present at a sufficiently high concentration to scavenge all of the $\text{HO}_2/\text{O}_2^{\cdot-}$ produced (7).

To determine whether reactions occurring at the lepidocrocite surface are acting as a source of $\text{HO}_2/\text{O}_2^{\cdot-}$, it is necessary to compare the rate of $\text{HO}_2/\text{O}_2^{\cdot-}$ production in the lepidocrocite suspensions to that expected from photo-oxidation of fulvic acid alone. However, this problem is not as straightforward as comparing hydrogen peroxide production rates in the two systems. As explained previously, because of a change in stoichiometry, up to twice as much hydrogen peroxide could be formed in the presence of Fe(II) than in its absence at the same $\text{HO}_2/\text{O}_2^{\cdot-}$ formation rate. [Previous experiments (27) indicate that the increase is approximately a factor of 1.5.] The hydrogen peroxide formation rate measured in the absence of added iron, $0.68 (\pm 0.03) \times 10^{-10} \text{ M s}^{-1}$ (given by a linear least squares fit of the pH 3 and pH 5 data in Figure 2), therefore implies that the $\text{HO}_2/\text{O}_2^{\cdot-}$ formation rate lies roughly between $0.7 \times 10^{-10} \text{ M s}^{-1}$ (assuming a 1:1 stoichiometry of hydrogen peroxide formed per $\text{HO}_2/\text{O}_2^{\cdot-}$) and $1.4 \times 10^{-10} \text{ M s}^{-1}$ (assuming a 1:2 stoichiometry).

To compare this range with the value observed in the γ -FeOOH suspensions, we must also correct for the difference in light conditions. Comparison of the absorption spectra of the solutions containing 10 mg/L SRFA alone and those containing 10 mg/L SRFA plus 40 μM γ -FeOOH indicates that, due to absorption of light by the γ -FeOOH, 10–40% fewer photons (depending on the wavelength of the photon) are available in the suspensions as compared to the particle-free solutions (27). (Scattering of light by γ -FeOOH was negligible.) The observed rate should therefore be 10–40% smaller in the presence of particles than the rate observed in their absence, putting a lower bound of $0.4 \times 10^{-10} \text{ M s}^{-1}$ and an upper bound of $1.2 \times 10^{-10} \text{ M s}^{-1}$ on our estimate of the formation rate of $\text{HO}_2/\text{O}_2^{\cdot-}$ in the suspensions from direct (Fe-independent) photo-oxidation of fulvic acid. The formation rate of $\text{HO}_2/\text{O}_2^{\cdot-}$ given by the model of the heterogeneous system at both pH 3 and pH 5 is $1.4 \times 10^{-10} \text{ M s}^{-1}$ (Table 1). At the end of 300 min then, between 0.4 and 1.8 μM $\text{HO}_2/\text{O}_2^{\cdot-}$ may have come from additional reactions taking place in the suspensions. Comparison of this range with the amount of Fe(III) reduced by LMCT reactions (9.1 μM on the iron oxide surface and 3.2 μM in solution at pH 3 and 4.3 and 2.9 μM , respectively, at pH 5; see Figure 7) indicates that the majority of the organic radicals produced by these reactions do not reduce oxygen to $\text{HO}_2/\text{O}_2^{\cdot-}$.

The leveling of hydrogen peroxide concentration with time is consistent with a constant formation rate and simultaneous degradation by increasing amounts of Fe(II). Sinks of hydrogen peroxide other than its reaction with dissolved Fe(II), such as reactions on the photo-excited lepidocrocite surface (33), or reaction with surface Fe(II) (36) do not appear to be a significant factor in this experimental system.

Environmental Significance

It is clear that both iron and light have an accelerating effect on the oxidation of humic substances by oxygen. Miles and Brezonik (1) have made direct observations of this effect; our results provide more details on the mechanisms involved (Figure 7). In addition to a dark process [in which Fe(III) is reduced to Fe(II)], we observe two photo-oxidation processes of fulvic acid. The first, which does not seem to require the presence of metals, results in reduction of oxygen to $\text{HO}_2/\text{O}_2^{\cdot-}$. The second process, photo-induced LMCT reaction of Fe(III)–fulvate complex, occurs both in solution and on the surface of iron oxide and results in the reduction of Fe(III). Dissolved Fe(III) is continuously supplied via re-oxidation of Fe(II) by both $\text{HO}_2/\text{O}_2^{\cdot-}$ and H_2O_2 . The HO^{\cdot} (or other strongly oxidizing) radicals produced by the reaction of Fe(II) with H_2O_2 further oxidize fulvic acid. Interestingly, neither the oxidation of fulvic acid nor the redox cycling of Fe is dominated by only one or two processes in our experimental systems. A question that remains to be answered is whether oxidation of humic substances in the presence of iron leads to different products (as well as faster oxidation) than oxidation in the absence of iron.

Because the rate constants determined for one fulvic acid and one iron oxide phase under certain light conditions cannot be expected to be generalizable, the question of the net effect of light and fulvic acid on iron redox states is more difficult to answer. Indeed both light-dependent acceleration of Fe(III) reduction (40–42) and Fe(II) oxidation (43) have been observed in the field. In general, the effects of light should diminish with depth in the water column as light in the UV and near-UV part of the spectrum is attenuated. In highly colored waters, the reactions described here may only be significant in the top few centimeters.

Although we did not observe substantial differences in the behavior of our experimental solutions between pH 3 and pH 5, this system would behave quite differently at higher pH. First, the ability of humic substances to complex dissolved Fe(III) could diminish as the free-ion activity of Fe(III) is lowered by hydrolysis. Formation of Fe(III)–humate complexes at the surfaces of iron oxides also decreases drastically with increasing pH (33). The significance of photochemical LMCT reactions involving humic substances could therefore be much decreased. A second difference is that $\text{HO}_2/\text{O}_2^{\cdot-}$, which oxidizes Fe(II) in our experimental systems, could instead become a significant reductant of Fe(III) at higher pH values, especially if the Fe(III) is not organically complexed (44).

Acknowledgments

We thank Stephan Hug for his help with Matlab and the kinetic modeling; Neil Blough, Silvio Canonica, Jürg Hoigné, René Schwarzenbach, David Sedlak, Werner Stumm, Oliver Zafiriou, and Yuogang Zuo for helpful discussions and comments; and Jerry Leenheer for providing us with a sample of fulvic acid.

Literature Cited

- (1) Miles, C. J.; Brezonik, P. L. *Environ. Sci. Technol.* **1981**, *15*, 1089–1095.
- (2) Zuo, Y.; Hoigné, J. *Environ. Sci. Technol.* **1992**, *26*, 1014–1022.
- (3) Faust, B. C.; Zepp, R. G. *Environ. Sci. Technol.* **1993**, *27*, 2517–2522.
- (4) King, D. W.; Lounsbury, H. A.; Millero, F. J. *Environ. Sci. Technol.* **1995**, *29*, 818–824.
- (5) Zepp, R. G.; Faust, B. C.; Hoigné, J. *Environ. Sci. Technol.* **1992**, *26*, 313–319.
- (6) Sedlak, D. L.; Hoigné, J. *Atmos. Environ.* **1993**, *27A*, 2173–2185.
- (7) Voelker, B. M.; Sulzberger, B. *Environ. Sci. Technol.* **1996**, *30*, 1106–1114.
- (8) Waite, T. D.; Morel, F. M. M. *J. Colloid Interface Sci.* **1984**, *102*, 121–137.

- (9) Balzani, V.; Carassiti, V. *Photochemistry of Coordination Compounds*; Academic Press: London, 1970.
- (10) Chateaufneuf, J.; Luszky, K. J.; Ingold, K. V. *J. Am. Chem. Soc.* **1988**, *110*, 2877–2893.
- (11) Blough, N. V.; Zepp, R. G. In *Active oxygen in chemistry*; Foote, C. S., Valentine, J. S., Eds.; Chapman and Hall: New York, 1995; pp 280–333.
- (12) von Sonntag, C.; Schuchmann, H.-P. *Angew. Chem. Int. Ed. Engl.* **1991**, *30*, 1229–1253.
- (13) Waite, T. D.; Morel, F. M. M. *Environ. Sci. Technol.* **1984**, *18*, 860–868.
- (14) Siffert, C.; Sulzberger, B. *Langmuir* **1991**, *7*, 1627–1634.
- (15) Tamura, H.; Goto, K.; Nagayama, M. *Corros. Sci.* **1976**, *16*, 197–207.
- (16) Sulzberger, B.; Laubscher, H. U. In *Aquatic Chemistry: Interfacial and Interspecies Processes*; Advances in Chemistry Series No. 244; Huang, C. P., O'Melia, C. R., Morgan, J. J., Eds.; American Chemical Society: Washington, DC, 1995; pp 279–290.
- (17) Cooper, W. J.; Zika, R. G.; Petasne, R. G.; Fischer, A. M. In *Aquatic Humic Substances: Influence on Fate and Treatment of Pollutants*; Suffett, I. H., MacCarthy, P., Eds.; American Chemical Society: Washington, DC, 1989; pp 333–362.
- (18) Hoigné, J.; Faust, B. C.; Haag, W. R.; Scully, F. E.; Zepp, R. G. In *Aquatic Humic Substances: Influence on Fate and Treatment of Pollutants*; Suffett, I. H., MacCarthy, P., Eds.; American Chemical Society: Washington, DC, 1989; pp 363–3817.
- (19) Sturzenegger, V. T. Ph.D. Dissertation No. 9004, Eidgenössische Technische Hochschule, Zürich, Switzerland, 1989.
- (20) Bielski, B. H. J.; Cabelli, D. E.; Arudi, R. L.; Ross, A. B. *J. Phys. Chem. Ref. Data* **1985**, *14*, 1041–1100.
- (21) Rush, J. D.; Bielski, B. H. J. *J. Phys. Chem.* **1985**, *89*, 5062–5066.
- (22) Deng, Y.; Stumm, W. *Appl. Geochem.* **1994**, *9*, 23–36.
- (23) Bondietti, G.; Sinniger, J.; Stumm, W. *Colloids Surf.* **1993**, *79*, 157–162.
- (24) Leenheer, J. A. *Environ. Sci. Technol.* **1981**, *15*, 578–587.
- (25) Schwertmann, U.; Cornell, R. M. *Iron oxides in the laboratory: preparation and characterization*; VCH Publishers, Inc.: New York, 1981.
- (26) Braun, W.; Herron, J. T.; Kahaner, D. K. *Int. J. Chem. Kinet.* **1988**, *20*, 51–62.
- (27) Voelker, B. M. Ph.D. Dissertation No. 10901, Eidgenössische Technische Hochschule, Zürich, Switzerland, 1994.
- (28) Bader, H.; Sturzenegger, V.; Hoigné, J. *Water Res.* **1988**, *22*, 1109–1115.
- (29) Skoog, D. A.; West, D. M. *Fundamentals of Analytical Chemistry*, 2nd ed.; Holt International: London, 1969.
- (30) Siffert, C. Ph.D. Dissertation No. 8852, Eidgenössische Technische Hochschule, Zürich, Switzerland, 1989.
- (31) Blough, N. V.; Zafiriou, O. C. *Inorg. Chem.* **1985**, *24*, 3502–3504.
- (32) Micinski, E.; Ball, L. A.; Zafiriou, O. C. *J. Geophys. Res.* **1993**, *98* (C2), 2299–2306.
- (33) Tipping, E. *Geochim. Cosmochim. Acta* **1981**, *45*, 191–199.
- (34) King, D. W.; Aldrich, R. A.; Charnecki, S. E. *Mar. Chem.* **1993**, *44*, 105–120.
- (35) Pehkonen, S. O.; Siefert, R.; Erel, Y.; Webb, S.; Hoffmann, M. R. *Environ. Sci. Technol.* **1993**, *27*, 2056–2062.
- (36) Aiken, G. R.; Brown, P. A.; Noyes, T. I.; Pinckney, D. J. In *Humic Substances in the Suwannee River, Georgia: Interactions, Properties, and Proposed Structures*; Averett, R. C., Leenheer, J. A., McKnight, D. M., Thorn, K. A., Eds.; U.S. Geological Survey Open File Report 87-557; U.S. Geological Survey: Denver, CO, 1989; pp 163–178.
- (37) Waite, T. D. *Rev. Mineral.* **1990**, *23*, 559–603.
- (38) Vinodgopal, K.; Kamat, P. V. *Environ. Sci. Technol.* **1992**, *26*, 1963–1966.
- (39) Sulzberger, B.; Laubscher, H. U. *Mar. Chem.* **1995**, *50*, 103–115.
- (40) Collienne, R. H. *Limnol. Oceanogr.* **1983**, *28*, 83–100.
- (41) McKnight, D. M.; Kimball, B. A.; Bencala, K. E. *Science* **1988**, *240*, 637–640.
- (42) Sulzberger, B.; Schnoor, J.; Giovanoli, R.; Hering, J. G.; Zobrist, J. *Aquat. Sci.* **1990**, *52*, 56–74.
- (43) Barry, R. C.; Schnoor, J. L.; Sulzberger, B.; Sigg, L.; Stumm, W. *Water Res.* **1994**, *28*, 323–333.
- (44) Voelker, B. M.; Sedlak, D. L. *Mar. Chem.* **1995**, *50*, 93–102.

Received for review May 6, 1996. Revised manuscript received November 1, 1996. Accepted November 20, 1996.[®]

ES9604018

[®] Abstract published in *Advance ACS Abstracts*, February 1, 1997.